 CMES, vol.35, no.3, pp.215-225, 2008

Strength Asymmetry of Twinned Copper Nanowires under Tension and Compression

Yongfeng Zhang[1], **Hanchen Huang**[1,2] **and Satya N. Atluri**[3]

Abstract: Molecular dynamics simulations reveal the asymmetrical yield strength of twinned copper nanowires under tension and compression. The simulation results show that the strength of nanowires depends on loading conditions, morphologies, and twin spacing. Under tensile loading condition the Schmidt factor of the leading partial is larger than that under compression. Effectively, the yield strength under tension is smaller than that under compression. When the cross-section is circular in morphology, dislocation nucleation requires larger stress, and the asymmetry of yield strength depends on the nucleation stress. When the cross section is square in morphology, dislocation nucleation requires smaller stress, and the asymmetry of yield strength depends on the stress of penetrating twin boundaries.

Keyword: Nanowire, twin, strength, dislocation, simulation

1 Introduction

Metallic nanowires are of great technological interest [Tian, Wang, Kurtz, Mallouk, and Chan (2003)]. As the scale of electronic devices becomes ever smaller, metallic nanowires are expected to be the building blocks as both interconnects and functional units in nanoelectromechanical systems [Husain, Hone, Postma, Huang, Drake, Barbic, Scherer, and Roukes (2003)]. Metallic nanowires are also useful in scanning tunneling microscope (STM) and atomic force microscope (AFM) for nanoscale tip-sample interactions [Tay and Thong (2004)]. Functionalities of these nanowires depend on their mechanical properties, which differ from those in bulk due to the presence of large free surface area. The elastic moduli and yield strength of metallic nanowires have strong dependence on lateral size [Zhou and Huang

[1] Department of Mechanical, Aerospace and Nuclear Engineering, Rensselaer Polytechnic Institute, Troy, NY 12180

[2] Corresponding author. Email: hanchen@rpi.edu

[3] Department of Mechanical and Aerospace Engineering, University of California Irvine, Irvine, CA 92612

(2004), Greer and Nix (2006)]. As a result of the surface stress, large asymmetry exists in the yield strength of gold nanowires under tension and compression [Diao, Gao, and Dunn (2004)]. Through a reversible crystallographic lattice reorientation, face-centered-cubic (FCC) metallic nanowires show rubber-like pseudoelastic and shape memory behavior [Liang, Zhou, and Ke (2005), Park, Gall, and Zimmerman (2005)]. The formation of twin boundary is common in FCC metallic nanowires due to its high symmetry and low formation energy. This planar defect forms during both synthesis [Wang, Huang, Kesapragada, and Gall (2005), Shim and Huang (2007)] and mechanical deformation [Park, Gall, and Zimmerman (2006), Zhou, Hsiung and Huang (2004)], further enriching the unique properties of metallic nanowires. For example, dislocations usually glide on $\{111\}$ planes in FCC metals like Cu. After penetrating a twin boundary in a <111> nanowire, a dislocation may glide on $\{100\}$ plane in the new grain [Wang and Huang (2006)]. Serving as obstacles of dislocation motion, twin boundaries may strengthen a metallic nanowire, as revealed by molecular dynamics simulations [Cao, Wei, and Mao (2007), Afanasyev and Sansoz (2007)].

In this work we report the yield strength asymmetry of twinned copper nanowires under uniaxial tension and compression. To examine the effect of morphology, we consider two types of cross-sections – circular and square. As described in an earlier report [Zhang and Huang (2008)], morphologies dictate whether yield strength varies with twin spacing. This paper focuses on the asymmetry in yield strength under tension and compression. In the following, we will start with the description of simulation method in section 2, then the simulation results in section 3. Finally we conclude in section 4.

2 Simulation details

Four elements of the simulation method are interatomic potential, setup of simulation cells, application of strain, and defect identification. The Mishin potential has been calibrated according to *ab initio* results of stacking fault and twin formation energy, and is therefore our choice for this study [Mishin, Mehl, Papaconstantopoulos, Voter, and Kress (2001)]. According to this embedded-atom-method (EAM) potential, the total potential energy of an atomic system can be written as:

$$U = \frac{1}{2}\sum_{ij} V(r_{ij}) + \sum_{i} F(\overline{\rho}_i) \tag{1}$$

Here $V(r_{ij})$ is a pair potential function of distance r_{ij} between atom i and atom j, and F is the embedding energy. $\overline{\rho}_i$ is the host electron density function induced at site i by all other atoms in the system. More details of the Mishin potential can be found elsewhere [Mishin, Mehl, Papaconstantopoulos, Voter, and Kress (2001)].

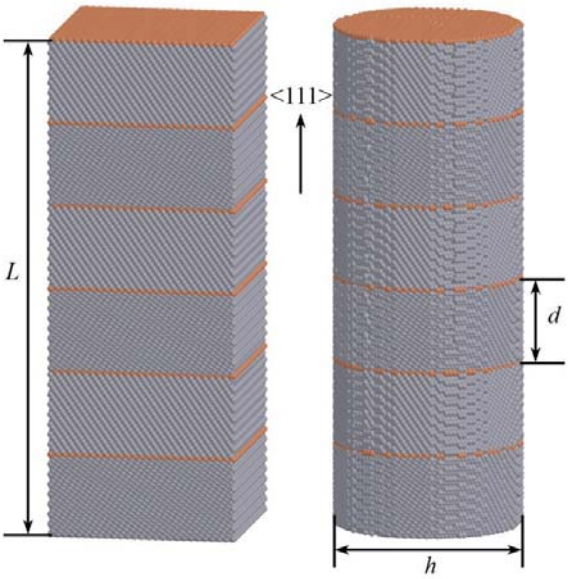

Figure 1: Schematic of twinned nanowires with square (left) and circular (right) cross-sections; gray spheres represent Cu atoms and orange spheres those Cu atoms in twin boundaries.

Two types of nanowires are considered in this work. As shown in fig. 1, a simulation cell contains a <111> orientated nanowire with either square (referred as square nanowire thereafter) or circular cross-section (circular nanowire). For square nanowires, the side surfaces are {110} and {112} to minimize the surface energy. For circular nanowires, the side surface is randomly cut from bulk lattice. For both types of nanowires, the length L in axial direction is 31 nm with periodic boundary condition applied in this direction. The lateral dimension h–side length for square nanowires and diameter for circular nanowires – is about 8 nm. The estimated buckling stress of fixed-ends columns of this dimension is much higher than the applied stress in our simulations; that is, the compressive deformation will not lead to buckling. The twin spacing d varies from 1.05 nm to 15.75 nm in the investigation of twin spacing effects. The simulation cells are first relaxed using conjugate gradient method [Golub and O'Leary (1989), Press, Teukolsky, Vetterling, and Flannery (1992)] to minimize the total energy and then equilibrated at 300K using the Nose-Hoover thermostat [Nose (1984), Hoover (1985)] for 25 ps (time step being 5 fs). After this equilibration process, the strain is applied by uniformly increasing (decreasing) the axial length by 0.1% of the original length every 12.5

ps. The corresponding tensile (compressive) engineering strain rate is 8×10^7/s. After each strain increment, the average virial stress [Diao, Gall, and Dunn (2004)] is calculated for the last 500 time steps. The use of virial stress has been discussed by several groups [Shen and Atluri (2004), Zhou (2003)]. When the average stress is concerned, as is the case here, the difference is unessential.

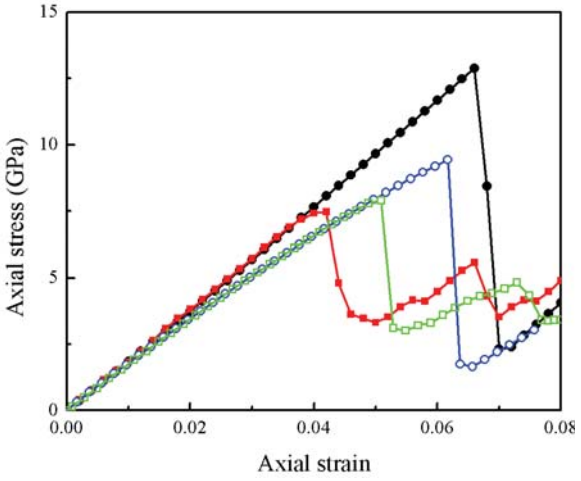

Figure 2: Stress-strain curves for circular (circles) and square (squares) nanowires under tension (open) and compression (solid).

The bond pair analysis method [Honeycutt and Anderson (1987)] is used to identify twin boundaries and dislocations. This method defines a pair distribution sequence consisting of three digit numbers for each pair of nearest neighbors. The first number is the number of common neighbors shared by the host pair of atoms; the second is the number of bonds formed between those common neighbors; and the last one represents the length of the longest chain formed by those bonds, in unit of the nearest neighbor distance. Each atom that has local FCC crystallinity forms twelve 421 pair sequences with its twelve nearest neighbors; while each hexagonal-close-packed (HCP) atom forms six 421 and six 422. Thus we can classify the atoms into three categories: those with FCC structures, those with HCP structures, and others. Twin boundaries are outlined by one layer of HCP atoms, stacking fault by two layers of HCP atoms, and dislocations by the "others".

3 Results and discussions

In presenting the simulation results, we first look at the overall behavior and then examine the atomic mechanism in details. In fig. 2 the stress-strain curves of

selected nanowires under tension and compression are plotted. Under increasing axial strain, the stress increases linearly before a sudden drop. The sudden drop in axial stress defines the yielding point in this work. Estimated from the initial linear part of the stress-strain curve, the Young's modulus is about 190 GPa for both types of nanowires in agreement with the results in literature [Cao, Wei, and Mao (2007)]. With increasing compressive (tensile) strain, the Young's modulus shows slight increase (decrease).

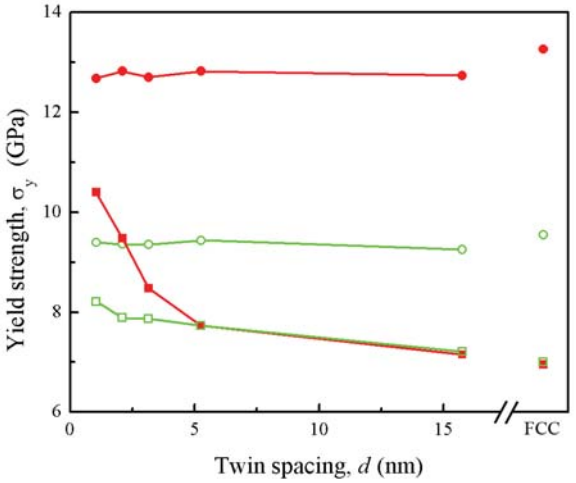

Figure 3: Yield strength σ_y of circular (circles) and square (squares) nanowires under tension (open) and compression (solid).

The yield strength σ_y of nanowires under tension and compression is shown in fig. 3. The yield strength asymmetry is prominent for circular nanowires (circular symbols in fig. 3), and the prominence is little affected by the twin spacing. For square nanowires this asymmetry becomes important only when the twin spacing is smaller than 5 nm. The variation of strength with twin spacing has been presented elsewhere [Zhang and Huang (2008)]; here we focus on the asymmetry in yield strength. To further understand this phenomenon, the necessary stress required for the first dislocation nucleation σ_n is also plotted in fig. 4. The asymmetry in σ_n corresponds to that in σ_y, for circular nanowires. This is logical, since dislocation nucleation requires large stress and dictates the yield strength for circular nanowires. In contrast, dislocation nucleation is easy for square nanowires due to the existence of corners, and the asymmetry in σ_n does not correspond to the asymmetry in σ_y.

To understand yield strength asymmetry, we analyze dislocation dynamics. FCC metallic nanowires deform through 1/2<110> full dislocations consisting of 1/6<112>

partials. While under uniaxial loading, the leading partial and the trailing have different Schmidt factors. As shown in table 1, for <111> oriented nanowires, the leading partial has smaller Schmidt factor under compression than that under tension. Since the resolved shear stress is proportional to the Schmidt factor, it is easier to nucleate a leading partial under tension than under compression, resulting in much higher dislocation nucleation stress σ_n and yield strength σ_y under compression. It should be noted that in <111> metallic nanowires the tensile surface stress favors compressive yielding [Diao, Gao, and Dunn (2004)]. In our cases, the axial contraction caused by surface stress is small and negligible.

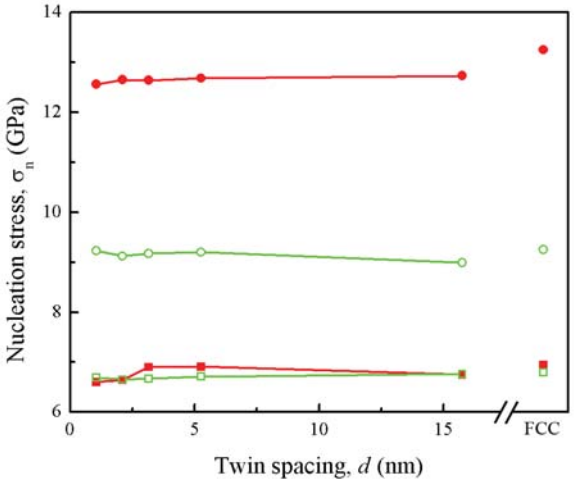

Figure 4: Dislocation nucleation stress σ_n of circular (circles) and square (squares) nanowires under tension (open) and compression (solid).

Table 1: Schmidt factors for <111> copper nanowires under tension and compression

Loading	**Tension**	**Compression**
Leading	0.31	0.16
Trailing	0.16	0.31

The Schmidt factor argument explains the yield strength asymmetry of circular nanowires. For square nanowires, the sharp edges make dislocation nucleation stress much lower. Therefore, the asymmetry does not exist when twin spacing is large. The easy nucleation of dislocation is directly correlated with atomic vibration amplitude [Zhu, Li, Samanta, Leach, and Gall (2008), Zuo, Ngan, and Zheng

(2005)]. As shown in fig. 5 for a square nanowire, atoms along the sharp edges have large amplitude of vibration up to 0.121 nm. In contrast, for a circular nanowire the largest amplitude of vibration is only 0.045 nm, which occurs at the intersections of twin boundaries and surfaces. The increased atomic vibration makes the dislocation nucleation much easier, resulting in a reduced strength, as shown in fig. 3 and fig. 4.

As twin spacing is below 5 nm, the asymmetrical yield strength of square nanowires is due to the strengthening effect and the difference in deformation mechanisms under tension and compression. As can be seen in fig. 3, the introduction of twin boundaries strengthens square nanowires. This strengthening effect exists under both tension and compression and shows no asymmetry. When the twin spacing becomes smaller than 5 nm, further strengthening emerges under compression and leads to yield strength asymmetry.

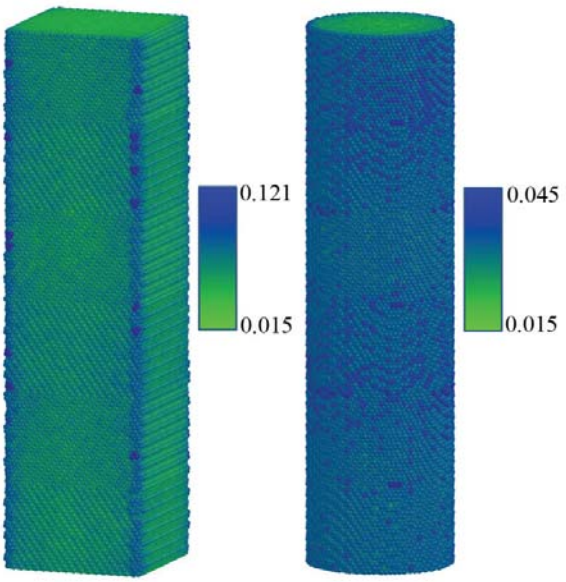

Figure 5: Atomic vibration amplitudes (in unit of nm) of square (left) and circular (right) nanowires; the twin spacing is 5.25 nm.

The dislocation dynamics in the yielding process of a square nanowire under compression is shown in fig. 6. Due to the large amplitude of atomic vibration, the first leading partial dislocation nucleates from a sharp edge; fig. 6(a). The trailing partial follows the leading one if there is enough room to expand the stacking fault between them [Yamakov, Wolf, Salazar, Phillpot, and Gleiter (2001)]. A full dis-

location will form at the twin boundary when the trailing partial arrives; fig. 6(b). After penetration, the new dislocation glides on a {100} plane with a Burgers vector of 1/2<110>, as shown in fig. 6(c). If the twin spacing becomes smaller than the equilibrium stacking fault splitting distance, which is several nanometer for copper [Yamakov, Wolf, Salazar, Phillpot, and Gleiter (2001)], the trailing dislocation has not nucleated when the leading partial reaches a twin boundary. In order to penetrate the twin boundary, the dislocation has to be full, requiring the arrival of the trailing dislocation. To overcome the repulsion between the leading and the trailing partials, additional stress is needed; this additional stress leads to higher strength under compression.

The same scenario should apply to the square nanowires under tension. Indeed, if a single dislocation is nucleated (top of fig. 7), the spacing between the leading and the trailing partials can be large. However, under tension, it happens that two leading partials nucleate on neighboring {111} planes at the same time. Their intersection or junction is sessile, forcing the two trailing dislocations to nucleate. Once the trailing dislocations form, they annihilate the junction formed by the two leading partials. In this process, the nucleation of trailing dislocation is independent of twin spacing.

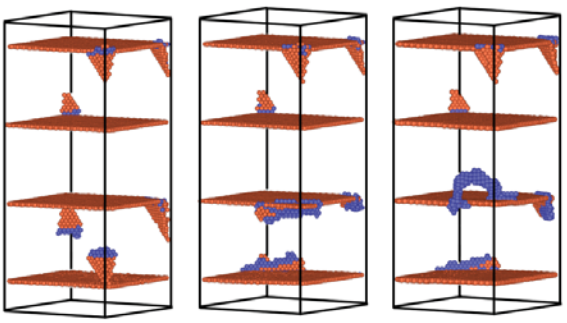

Figure 6: Atomic configurations of a square nanowire under compression showing dislocation (a) nucleation, (b) absorption by a twin boundary, and (c) penetration through a twin boundary; the twin spacing is 5.25 nm. Orange spheres represent atoms in HCP structure, and purple spheres other atoms; FCC atoms are removed for clarity.

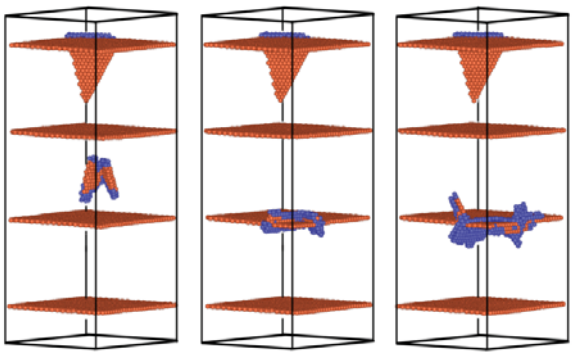

Figure 7: Atomic configurations of a square nanowire under tension showing dislocation (a) nucleation, (b) absorption by a twin boundary, and (c) penetration through a twin boundary; the twin spacing is 5.25 nm. Orange spheres represent atoms in HCP structure, and purple spheres other atoms; FCC atoms are removed for clarity.

4 Conclusions

In conclusion, our molecular dynamics simulations have revealed a yield strength asymmetry of twinned nanowires. For twinned Cu nanowires of circular cross-sections, the yield strength depends on dislocation nucleation stress, and it is higher under compression than that under tension. The asymmetry is a result of different Schmidt factors for leading partial dislocations under tension and compression. For twinned Cu nanowires of square cross-sections, the yield strength depends on the stress necessary for dislocation penetration of twin boundaries. As a result, there is little asymmetry when twin spacing is large. At small twin spacing (below 5 nm), the necessity of overcoming repulsion of leading and trailing partials in the nucleation of trailing partial leads to higher strength under compression; this is unnecessary under tension due to the sessile dislocation formation.

Acknowledgement: The authors gratefully acknowledge the financial support from National Science Foundation (CMMI-0739576, 0727413, and 0553300).

Reference

Afanasyev, K. A.; Sansoz, F. (2007): Strengthening in gold nanopillars with nanoscale twins. *Nano Lett.*, vol. 7, pp2056-2062.

Cao, A. J.; Wei, Y. G.; Mao, S. X. (2007): Deformation mechanisms of face-

centered-cubic metal nanowires with twin boundaries. *Appl. Phys. Lett.*, vol. 90, pp151909-151911.

Diao, J.; Gall, K.; Dunn, M. L. (2004): Atomistic simulation of the structure and elastic properties of gold nanowires. *J. Mech. Phys. Solids*, vol. 52, pp1935-1962.

Diao, J.; Gao, K.; Dunn, M. L. (2004): Yield strength asymmetry in metal nanowires. *Nano Lett.*, vol. 4, pp1863-1867.

Golub, G. H.; O'Leary, D. P. (1989): Some history of the conjugate gradient and laczos algorithms: 1948-1976. *SIAM review*, vol. 31, pp50-103.

Greer, J. R.; Nix, W. D. (2006): Nanoscale gold pillars strengthened through dislocation starvation. *Phys. Rev. B*, vol. 73, pp245410-245415.

Hirth, J. P.; Lothe, J. (1992): *Theory of dislocations*, the second edition, Krieger Publishing, UK.

Honeycutt, J. D.; Andersen, H. C. (1987): Molecular dynamics study of melting and freezing of small Lennard-Jones clusters, *J. Phys. Chem.*, Vol. 91, pp4950-4963.

Hoover, W. G. (1985): Canonical dynamics: Equilibrium phase-space distributions. *Phys. Rev. A*, vol. 31, pp1695-1697.

Husain, A.; Hone, J.; Postma, H. W. C.; Huang, X. M. H.; Drake, T.; Barbic M.; Scherer, A.; Roukes, M. L. (2003): Nanowire-based very-high-frequency electromechanical resonator. *Appl. Phys. Lett.*, vol. 83, pp1240-1242.

Liang, W.; Zhou, M.; Ke, F (2005): Shape memory effect in Cu nanowires. *Nano Lett.*, vol. 5, pp2039-2043.

Mishin, Y.; Mehl, M. J.; Papaconstantopoulos, D. A.; Voter, A. F.; Kress, J. D. (2001): Structural stability and lattice defects in copper: *Ab initio*, tight-binding, and embedded-atom calculations. *Phys. Rev. B*, vol. 63, pp224106-1-16.

Nosé, S. (1984): A unified formulation of the constant temperature molecular dynamics methods. *J. Chem. Phys.*, vol. 81, pp511-519.

Park, H. S.; Gall, K.; Zimmerman, J. A. (2005): Shape Memory and Pseudoelasticity in Metal Nanowires. *Phys. Rev. Lett.*, vol. 95, pp255504-1-4.

Park, H. S.; Gall, K.; Zimmerman, J. A. (2006): Deformation of FCC nanowires by twinning and slip. *J. Mech. Phys. Solids*, vol. 54, pp1862-1881.

Press, W. H.; Teukolsky, S. A.; Vetterling, W. T.; Flannery, B. P. (1992): *Numerical recipes in FORTRAN 77: The art of scientific computing, Second edition*. Cambridge University Press, USA.

Shen, S; Atluri, S. N. (2004): Atomic-level stress calculation and continuum-molecular system equivalence. *CMES: Computer Modeling in Engineering & Sceinces*,

vol. 6, pp91-104.

Shim, H. W.; Huang, H. C. (2007): Three-stage transition during silicon carbide nanowire growth. *Appl. Phys. Lett.*, vol. 90, pp083106-083108.

Tay, A. B. H.; Thong, J. T. L. (2004): High-resolution nanowire atomic force microscope probe grown by a field-emission induced process. *Appl. Phys. Lett.*, vol. 84, pp5207-5209.

Tian, M.; Wang, J.; Kurtz, J.; Mallouk, T. E.; Chan, M. H. W. (2003): Electrochemical growth of single-crystal metal nanowires via two-dimensional nucleation and growth mechanism. *Nano Lett.*, vol. 3, pp919-923.

Wang, J.; Huang, H. C. (2006): Novel deformation mechanism of twinned nanowires. *Appl. Phys. Lett.*, vol. 88, pp203112-203114.

Wang, J.; Huang, H. C.; Kesapragada, S. V.; Gall, D. (2005): Growth of Y-shaped nanorods through physical vapor deposition. *Nano Lett.*, vol. 5, pp2505-2508.

Yamakov, V.; Wolf, D.; Salazar, M.; Phillpot, S. R.; Gleiter, H. (2001): Length-scale effects in the nucleation of extended dislocations in nanocrystalline Al by molecular-dynamics simulation. *Acta Mater.*, vol. 49, pp2713-2722.

Zhang, Y. F.; Huang, H. C. (2008): Do twin boundaries always strengthen nanowires? *Nanoscale Research Letters*, Accepted; DOI: 10.1007/s11671-008-9198-1.

Zhou, L. G.; Huang, H. C. (2004): Are surfaces elastically softer or stiffer? *Appl. Phys. Lett.*, vol. 84, pp1940-1942.

Zhou, L. G.; Hsiung, L. M.; Huang H. C. (2004): Nucleation and propagation of deformation twin in polysynthetically twinned TiAl. *CMES: Computer Modeling in Engineering & Sceinces*, vol. 6, pp.245-252.

Zhou. M. (2003): A new look at the atomic level virial stress: on continuum-molecular system equivalence. *Proc. R. Soc. Lond. A* 459, pp2347-2392.

Zhu, T.; Li, J.; Samanta, A.; Leach, A.; Gall, K. (2008): Temperature and Strain-Rate Dependence of Surface Dislocation Nucleation. *Phys. Rev. Lett.*, vol. 100, pp025502-1-4.

Zuo, L.; Ngan, A. H. W.; Zheng, G. P. (2005): Size dependence of inceipient dislocations plasticity in Ni_3Al. *Phys. Rev. Lett.*, vol. 94, pp095501-1-4.